PROCEEDINGS OF SCIENCE

ONLINE ICRC 2021
THE ASTROPARTICLE PHYSICS CONFERENCE
Berlin | Germany
37th International Cosmic Ray Conference
12–23 July 2021

Technological options for the Southern Wide-field Gamma-ray Observatory (SWGO) and current design status

Felix Werner[a,*] **and Lukas Nellen**[b] **on behalf of the SWGO Collaboration**
(a complete list of authors can be found at the end of the proceedings)

[a] *Max-Planck-Institut für Kernphysik,*
Postfach 103980, 69029 Heidelberg, Germany
[b] *Universidad Nacional Autónoma de México,*
Instituto de Ciencias Nucleares, Mexico City, Mexico
E-mail: felix.werner@mpi-hd.mpg.de, lukas@nucleares.unam.mx

The SWGO Collaboration is in the process of designing and prototyping a wide field of view, high duty cycle complement to CTA and the existing ground-based particle detectors of the Northern Hemisphere (HAWC and LHAASO). In this contribution, we will compare the various technological options for designing the detector and present an overarching system design accommodating them. We will introduce a feasible reference configuration that is used for the first large-scale simulations and cost estimates, and show ongoing prototyping work focused on reaching a maintenance-free and cost-effective detector.

37th International Cosmic Ray Conference (ICRC 2021)
July 12th–23rd, 2021
Online – Berlin, Germany

*Presenter

PoS(ICRC2021)714

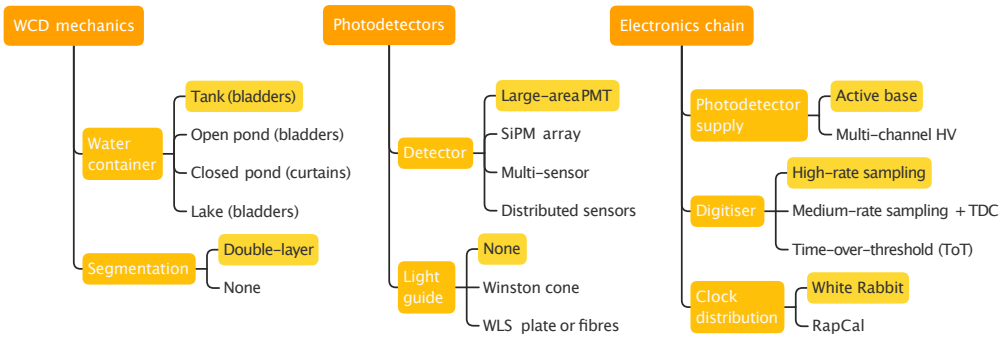

Figure 1: Decomposition of the detector into its main components and options. Reference choices for the individual components are highlighted. The options are discussed in the following sections of the main text.

1. Introduction and system architecture

The SWGO aims to augment the major ground-based, wide-field, high duty-cycle gamma-ray observatories HAWC [1] and LHAASO [2] with a new detector on the Southern Hemisphere, to be deployed at a high-altitude site in the South American Andes. The observatory aims to cover a wide energy range from around 100 GeV to the PeV scale. At low energies, a high detector altitude, particle detection efficiency, and hadron rejection efficiency are major design drivers. The energy reach is given by the effective area covered by the detector with sufficient energy resolution and hadron rejection efficiency, which—given limited funds—must be ensured with minimal coverage.

The concept currently serving as a baseline for the ongoing developments consists of a dense core array (~80% fill factor) covering a circular area of 160 m radius, surrounded by a sparse array of outriggers (~5% fill factor) up to a radius of 300 m. The detector units are water Cherenkov detectors (WCDs)—optically isolated volumes of pure water instrumented with photosensors to measure the time and particle energy density of the shower front. Hadronic background may be rejected based on characteristics of the measured particle density profile and by identifying muon-like signatures.

The choices for the detector concept and its components—the details of the individual detector unit design, photosensors and electronics—are still under consideration. To support prototyping of different options, the detector has been decomposed as shown in Fig. 1. To aid convergence towards the end of the R&D phase, the set of options to investigate and a specific configuration that may be used as a reference for comparing the cost and performance of these options has been agreed upon.[1] The components of this *reference configuration* have been chosen based on flexibility (favouring components that are less constraining on the site characteristics), feasibility (favouring low-risk technologies), and technical readiness (favouring components that may be costed now).

Due to the comparatively large scale and inherent remoteness of the detector, one particular focus is to reduce the high-altitude labour needed for deployment and operation. The goal is to build a detector that retains its target performance over its full life cycle of at least 10 years with little or no maintenance.

A general overview of the project and related activities is given in Ref. [3] of these proceedings. In the following, the options that are being considered for the detector concept and the individual detector components are discussed, and the reference choices are motivated.

[1]The array layout and detector unit dimensions are also part of that reference configuration and subject to optimisation.

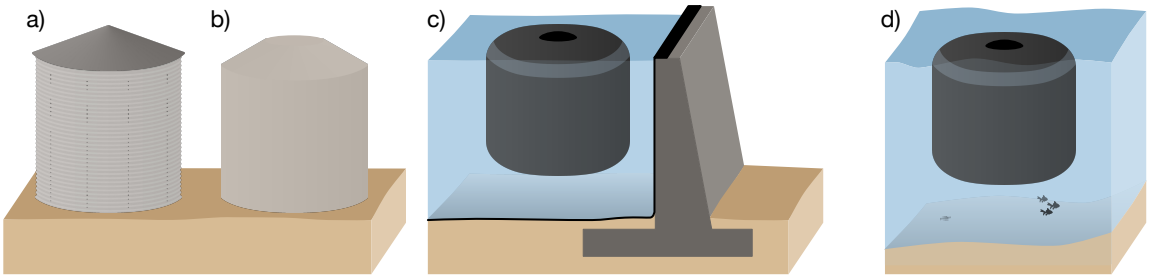

Figure 2: Detector concepts under study: cylindrical tanks constructed from **(a)** corrugated steel sheets or **(b)** roto-moulded HDPE; **(c)** open pond with floating bladder; **(d)** natural lake with floating bladder.

2. Detector concept

Three approaches are being considered for the construction of the core detector array (cf. Fig. 2):

- cylindrical tanks containing bladders
- bladders floating in artificial ponds
- bladders floating at or just below the surface of a natural lake

In each of these, the bladders are made from a multi-layer material that is light-tight, does not pollute the contained water, provides sufficient tensile strength, and has a well-defined inner reflectivity for the relevant wavelengths and incidence angles. Hence, a common material may be developed, with variations mostly for the specific mechanical requirements of the different approaches.

The three approaches provide different trade-offs in terms of required labour and materials for construction. Furthermore, some options may only be realised cost-effectively at certain sites. In the following, a brief overview of the three approaches is given.

Tanks

An array of tanks such as HAWC has the fewest restrictions on site characteristics. Ground needs to be levelled only at the scale of the tank surface, the array layout may be adapted, e.g., to avoid areas that would be particularly expensive to clear or grade. Water run-off needs to be considered.

Two options are being considered for the tank material: corrugated steel sheets assembled on site and roto-moulded HDPE. For steel tanks, a thick geotextile may protect the bladder from the ground surface, and a slanted roof carries potential snow load. The packed sheets are cost-effective to ship even from abroad, but require some assembly labour at the (high-altitude) site. On the other hand, HDPE tanks have to be produced (via convection-based roto-moulding) in the vicinity of the destination to become cost-effective. For these, a deployment model similar to that of the Surface Detector of the Pierre Auger Observatory [4] could be adopted: tanks could be fully prepared at a low-altitude site and shipped to their final destination with installed bladder and photosensors. Production and transport restrictions may limit any dimension of such a tank to ~4 m.

For a dense array of tanks, deployment and access have to be considered when planning the layout. For cylindrical tanks, average fill factors of 80% appear feasible.

Quotations available for both options suggest similarly high purchase costs when comparing steel sheets shipped to the nearest port and HDPE tanks produced at a specially set-up plant over the course of a few years. Bladders may be significantly thinner than for the other concepts.

Artificial ponds

As an alternative to a dense array of individual tanks, artificial ponds could be constructed with concrete walls and lined for water-tightness. Multiple ponds of $O(10\,000\,\mathrm{m}^2)$ each would be favoured over one large pond to support a modular construction. Two designs may be considered: a single water volume covered with a light-tight roof and with detector units optically decoupled with curtains (as in LHAASO); or individual light-tight and water-tight bladders floating in open water. A nearby water source is needed in both cases to replenish evaporated or otherwise leaked water. An open pond may also need an overflow channel and would therefore benefit from a nearby river.

Considering the challenges of making large buildings light-tight and of maintaining the quality of a large water body in contact with air, the bladder-based approach currently appears more promising. Both approaches require a significant amount of civil engineering to be studied and optimised with local partners, and can likely only be cost-effective if decommissioning is not needed, e.g., if the local community can repurpose the reservoirs after the project has concluded.

If the dense core array is built using ponds, a potential sparse array of surrounding outriggers may be realised using somewhat smaller ponds, or clustered or regularly spaced tanks (depending on the conditions at a specific site and a cost/performance optimisation).

Natural lakes

Peru hosts several high-altitude lakes with road access and km^2-scale parts of sufficient depth to float light-tight bladders at the surface. This approach requires the least amount of civil engineering and material to contain the bladders, and it may be feasible to fill the bladders with purified lake water (avoiding water transport costs). Hence, a lake-based detector could become very cost-effective if the engineering challenges associated with the construction, and stabilisation and deployment of the bladders in the open water can be addressed effectively, see Ref. [5] for more details.

3. Unit design

Two main concepts for the dense core detector are being pursued in the collaboration: deep double-layer WCDs (DLWCDs) and shallow multi-channel WCDs.

DLWCDs with one photosensor per layer provide a calorimetric measurement of the electromagnetic component in the upper layer and muon counting in the lower layer. [6] The upper layer has to be several radiation lengths deep to keep the electromagnetic particles from punching through to the muon compartment; a depth of ~2.5 m seems to be adequate to tag muons in the lower layer with sufficient purity [7]. If the lower compartment is lined with highly reflective, matte material such as Tyvek, a depth of 50 cm is already sufficient—suggesting a minimum total depth of 3 m for this type of detector. The particle detection efficiency of the upper layer is then mostly dictated by its width, the effective area of the photosensor, and the reflectivity of the wall material, and thus subject to cost/performance optimisation. Additionally, the choice of wall materials for the upper layer presents a trade-off between a higher detection efficiency (highly reflective walls) and a clean time signature of the detected photons (non-reflective walls). Preliminary studies taking into account the skew of the arrival time distribution of the first detected photon in a likelihood-based direction fit indicate that a reduced energy threshold may be reached using reflective walls with no significant degradation in angular resolution compared to units with non-reflective walls [7].

A cylindrical, 3.8 m diameter DLWCD with Tyvek-lined walls in the 2.5 m deep upper layer and a 0.5 m deep lower layer entirely lined with Tyvek—both equipped with a central 8-inch high-QE photo-multiplier tube (PMT) at the opaque layer separator—provides good overall performance and can be realised cost-effectively with steel and HDPE tanks, and in lake-based and pond-based detectors. Hence, this design has been selected to be used for the reference configuration.

An alternative design comprised of WCDs with a single, shallow compartment equipped with four photosensors may distinguish muons from electromagnetic particles based on the charge asymmetry and rise times of the signals within one detector unit. Simulations of an array of Tyvek-lined WCDs with a mere depth of 1.7 m have shown promising results for muon identification and γ-hadron discrimination [8].

These designs represent different cost trade-offs between required detector and water volume, and the number of electronics channels. Efforts are ongoing to define arrays of both detector types with similar nominal costs for performance comparisons in the second half of SWGO's R&D phase.

The unit designs mentioned above may not be best suited for a sparse outrigger array: the muon tagging purity of isolated DLWCDs is affected by side entry into the muon compartment, and the high channel count of shallow WCDs increases cabling costs. Studies are planned to compare the cost and performance of simpler single-channel WCDs to that of clusters of $O(60)$ detector units (with potentially shielded edges) with overall reduced side-entry and cable lengths.

4. Photosensors and electronics chain

While mass-produced SiPMs have become cheaper in recent years, large-area vacuum PMTs still provide the lowest cost per effective photo-active area and are simpler to interface than SiPM arrays. PMTs also show significantly lower dark count rates per effective area, potentially allowing a lower threshold for an array-level coincidence trigger. Hence, PMTs have been selected for the reference configuration while technological advancements of SiPM arrays are being closely followed.

Large-area PMTs, operated at a high gain to enable the detection of single photo-electrons and to reduce transit-time jitter, tend to provide only a limited range for which the output peak current grows linearly with (instantaneously) injected charge. Saturated detectors near the shower core need to be treated carefully to avoid biasing the reconstruction of shower geometry and energy. The enhanced photo-electron yield due to reflective walls shift the onset of non-linearities to somewhat lower energies, but the longer time profiles—lowering the peak photo-electron current—need to be considered when modelling this. Current lab efforts focus on deriving phenomenological models of candidate PMTs and the electronics response for early inclusion into the detector simulations. If studies indicate that saturation effects limit the detector performance, additional readout channels for intermediate dynodes or smaller photosensors may be considered.

The current assumption is that the PMTs are acquired from the manufacturer fully encapsulated, with either a standard passive base and HV-proof coaxial cable or an active base (integrating the generation of HV) and differential cable transmitting the analogue signal to a nearby data acquisition (DAQ) node housing digitisers and White-Rabbit slaves for precision timing. The concept is depicted in Fig. 3 for the case of passive-base photosensors. This modular approach has the advantage of housing most of the active electronics in accessible locations, aiding potential repair and maintenance efforts, and enabling later upgrades.

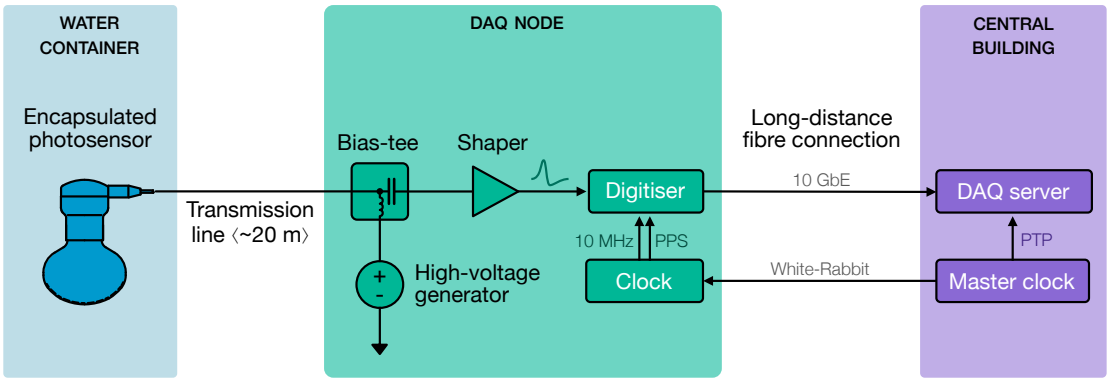

Figure 3: Architecture of the node-based design with encapsulated, passive-base photosensors phantom-powered via a coaxial transmission lines. Signal pick-offs (bias-tees), HV supplies, digitisers, and array timing modules are housed in DAQ nodes distributed throughout the array, each serving several tens of WCDs. A node is connected to the central infrastructure merely with single-mode fibres and AC power.

5. Data acquisition and trigger

For digitisation of the photosensor signals, high-frequency ADCs are being favoured over simpler time-over-threshold systems because of the benefits of sampled waveforms in linearity and (lack of) slewing, and the ability to reconstruct quantities based on the time profile which may be useful for particle discrimination. Based on the experience with the HAWC Outriggers [9], 250 MS s^{-1} 12-bit ADCs are expected to provide sufficient resolution in reconstructed timing and charge and are therefore selected for the reference configuration. To increase the dynamic range beyond the ~10^3 photo-electrons achieved with the HAWC Outriggers without increasing the channel count, non-linear pulse shaping methods are currently being studied. Furthermore, lower-rate ADCs augmented with GHz TDCs tagging the leading edge of a signal are being considered as alternatives.

The current working hypothesis for the data flow is shown in Fig. 4. Local triggering is expected to occur on the level of a single channel, ideally at sub-p.e. threshold. Based on detector simulations considering the high-altitude particle flux [10], the high particle detection efficiency of a reference unit (reaching already ~60% for 10 MeV photons [7]) leads to trigger rates of the order of 20–25 kHz for each upper-layer PMT. The resulting data rates of up to ~15 Mbit s^{-1} per channel [2] may be aggregated and handled by standard 10 GbE networking components and commodity servers for the data acquisition, signal reconstruction, and calibration. Such a design provides clean interfaces and a high degree of flexibility to apply optimal algorithms for pulse shape analysis, and allows array-level triggering based on the full pulse-level information purely in software.[3]

6. Prototyping efforts

Current prototyping efforts focus mostly on the critical items that have been identified so far. The aim is to build and operate prototypes for critical components and to collect sufficient data to

[2] Assuming 250 MS s^{-1} ADCs transferring 24 16-bit samples plus 96-bit waveform header per trigger on average.

[3] Assuming 128 bits per pulse, of the order of 30 Gbit s^{-1} will need to be processed by a software array trigger handling 6,000 DLWCDs. A simple coincidence trigger may process that amount of data on a commodity single-socket server. More sophisticated trigger algorithms may be realised by distributed and/or heterogeneous computing.

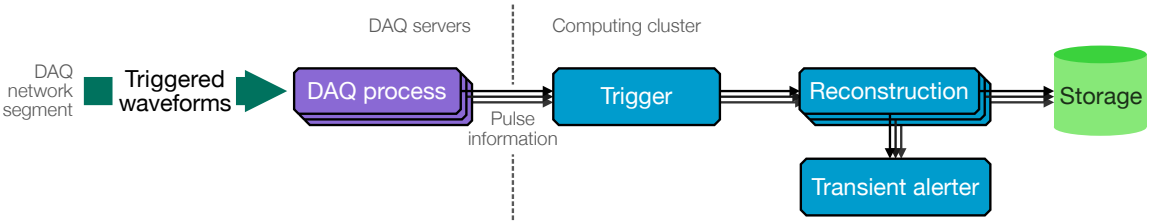

Figure 4: Working assumption for the flow of event information. Waveforms triggered at channel level with a low threshold are transferred from the frontends via conventional networking components. Pulse extraction and calibration are performed on dedicated DAQ servers, reducing waveforms to charge and timing quantities. All channel-level quantities are aggregated at a software process calculating an array-level trigger decision, building and forwarding array events to the distributed on-line event reconstruction and classification. Relevant data is then forwarded to a transient-alert generator and on-site storage.

choose between candidate designs towards the end of the R&D programme. Some examples of issues considered critical and the prototyping efforts to address these are given below.

Reliability of electronics and maintenance at high-altitude sites

Experience at the HAWC site has shown that some commercial electronics is not suited to operate at high-altitude sites, degrading or failing well before the advertised MTBF. To assess the reliability of candidate devices in realistic environmental conditions, test setups are being planned at candidate sites and at the HAWC site. For instance, a small-scale prototype DAQ node is being prepared for installation in Imata, Peru—one of the candidate sites with available infrastructure. The node will initially consist of the following components:

- Earthquake-tolerant, weather-proof, UV-proof, and dust-tight 19-inch cabinet
- environmental stabilisation with low-maintenance heat exchanger and dehumidifier
- dual-redundant power supplies and industrial 10 GbE switch
- custom 250 MS s^{-1} ADC system with GbE readout
- custom phantom HV supply and signal pick-off

Once established, the on-site setup may be completed with White Rabbit-based timing nodes and calibration devices, and further serve as a test bed for alternative components when prototypes are available. While the small-scale prototype DAQ node is designed to support only a limited number of electronics channels, all components should be suitable to operate in a potential larger-scale pathfinder that may help to further increase confidence in the components and the design.

Double-layer mechanics for tank-based detectors

For tank-based detectors, a mechanically robust and easy to deploy double-layer mechanics needs to be designed. A steel tank of 4 m diameter will be assembled at the HAWC site to develop and verify the mechanical design of the interior together with the experienced HAWC crew and to test the DLWCD's response in coincidence with the HAWC array. The proposed design will then be replicated and installed in the test tanks in South America.

Bag construction, stabilisation, and tracking for lake-based detectors

For lake-based detectors, a bag construction with interconnections that moderate and tolerate the wave-load and are easy to deploy needs to be designed. An open water tank with a capacity of 500 m^3

has been built at MPIK to act as a small-scale test bed for studying bag designs, interconnections, and deployment methods—see Ref. [5] in these proceedings for details. In addition, methods for tracking the position of the bags within the array and of the photosensors within the bags—both relevant for the angular resolution of the detector—may be evaluated in this context.

7. Outlook

The first large-scale simulations have been done based on the reference configuration described above, and shower reconstruction algorithms are currently being adapted to derive realistic performance curves. To be able to perform fair comparisons of the different options, e.g., for the detector mechanics, the main focus currently lies on developing cost models.

In parallel, the deployment of the small-scale prototype DAQ node to evaluate the reliability and operation of candidate devices in realistic conditions is targeted for the next austral summer. Because of the modular approach chosen for the electronics chain, this should enable the collaboration to eventually evaluate all proposed electronics options in this environment and to start developing the data processing stages, the software-based array trigger, and tools for data quality monitoring.

Acknowledgments

The SWGO Collaboration acknowledges the support from the agencies and organizations listed here: https://www.swgo.org/SWGOWiki/doku.php?id=acknowledgements. LN acknowledges UNAM PAPIIT IN110621 for support.

References

[1] A. U. Abeysekara *et al.* [HAWC], Astrophys. J. **881** (2019), 134. 10.3847/1538-4357/ab2f7d.

[2] C. Zhen *et al.* [LHAASO], Chin. Astron. Astrophys. **43** (2019), 457–478. 10.1016/j.chinastron.2019.11.001.

[3] J. Hinton, PoS **ICRC2021** (tbc), 023. https://pos.sissa.it/395/023/.

[4] I. Allekotte *et al.* [The Pierre Auger Collaboration], Nucl. Instrum. Meth. A **586** (2008), 409–420. 10.1016/j.nima.2007.12.016.

[5] H. Göksu and W. Hofmann, PoS **ICRC2021** (tbc), 708, https://pos.sissa.it/395/708/.

[6] A. Letessier-Selvon, P. Billoir, M. Blanco, I. C. Mariş and M. Settimo, Nucl. Instrum. Meth. A **767** (2014), 41–49. 10.1016/j.nima.2014.08.029.

[7] S. Kunwar, PoS **ICRC2021** (tbc), 902. https://pos.sissa.it/395/902/.

[8] R. Conceição, PoS **ICRC2021** (tbc), 707. https://pos.sissa.it/395/707/.

[9] V. Marandon, A. Jardin-Blicq and H. Schoorlemmer, PoS **ICRC2019** (2020), 736. 10.22323/1.358.0736.

[10] T. Sato, PLOS ONE **11(8)** (2016), e0160390. 10.1371/journal.pone.0160390.

Full Authors List: SWGO Collaboration

P. Abreu[1], A. Albert[2], E. O. Angüner[3], C. Arcaro[4], L. H. Arnaldi[5], J. C. Arteaga-Velázquez[6], P. Assis[1], A. Bakalová[7], U. Barres de Almeida[8], I. Batković[4], J. Bellido[9], E. Belmont-Moreno[10], F. Bisconti[11], A. Blanco[1], M. Bohacova[7], E. Bottacini[4], T. Bretz[12], C. Brisbois[13], P. Brogueira[1], A. M. Brown[14], T. Bulik[15], K. S. Caballero Mora[16], S. M. Campos[17] A. Chiavassa[11], L. Chytka[7], R. Conceição[1], G. Consolati[18], J. Cotzomi Paleta[19], S. Dasso[20], A. De Angelis[4], C. R. De Bom[8], E. de la Fuente[21], V. de Souza[22], D. Depaoli[11], G. Di Sciascio[23], C. O. Dib[24], D. Dorner[25], M. Doro[4], M. Du Vernois[26], T. Ergin[27], K. L. Fan[13], N. Fraija[8], S. Funk[28], J. I. García[17], J. A. García-González[29], S. T. García Roca[9], G. Giacinti[30], H. Goksu[30], B. S. González[1], F. Guarino[31], A. Guillén[32], F. Haist[30], P. M. Hansen[33], J. P. Harding[2], J. Hinton[30], W. Hofmann[30], B. Hona[34], D. Hoyos[17], P. Huentemeyer[35], F. Hueyotl-Zahuantitla[16] A. Insolia[36], P. Janecek[7], V. Joshi[28], B. Khelifi[37], S. Kunwar[30], G. La Mura[1], J. Lapington[38], M. R. Laspiur[17], F. Leitl[28], F. Longo[39], L. Lopes[1], R. Lopez-Coto[4], D. Mandat[7], A. G. Mariazzi[33], M. Mariotti[4], A. Marques Moraes[8], J. Martínez-Castro[40], H. Martínez-Huerta[41], S. May[42], D. G. Melo[43], L. F. Mendes[1], L. M. Mendes[1], T. Mineeva[24], A. Mitchell[44], S. Mohan[35], O. G. Morales Olivares[16], E. Moreno-Barbosa[19], L. Nellen[45], V. Novotny[7], L. Olivera-Nieto[30], E. Orlando[39], M. Pech[7], A. Pichel[20], M. Pimenta[1], M. Portes de Albuquerque[8], E. Prandini[4], M. S. Rado Cuchills[9], A. Reisenegger[46], B. Reville[30], C. D. Rho[47], A. C. Rovero[20], E. Ruiz-Velasco[30], G. A. Salazar[17], A. Sandoval[10], M. Santander[42], H. Schoorlemmer[30], F. Schüssler[48], V. H. Serrano[17], R. C. Shellard[8], A. Sinha[49], A. J. Smith[13], P. Surajbali[30], B. Tomé[1], I. Torres Aguilar[50], C. van Eldik[28], I. D. Vergara-Quispe[33], A. Viana[22], J. Vícha[7], C. F. Vigorito[11], X. Wang[35], F. Werner[30], R. White[30], M. A. Zamalloa Jara[9]

[1] Laboratório de Instrumentação e Física Experimental de Partículas (LIP), Av. Prof. Gama Pinto 2, 1649-003 Lisboa, Portugal
[2] Physics Division, Los Alamos National Laboratory, P.O. Box 1663, Los Alamos, NM 87545, United States
[3] Aix Marseille Univ, CNRS/IN2P3, CPPM, 163 avenue de Luminy - Case 902, 13288 Marseille cedex 09, France
[4] University of Padova, Department of Physics and Astronomy & INFN Padova, Via Marzolo 8 - 35131 Padova, Italy
[5] Centro Atómico Bariloche, Comisión Nacional de Energía Atómica, S. C. de Bariloche (8400), RN, Argentina
[6] Universidad Michoacana de San Nicolás de Hidalgo, Calle de Santiago Tapia 403, Centro, 58000 Morelia, Mich., México
[7] FZU, Institute of Physics of the Czech Academy of Sciences, Na Slovance 1999/2, 182 00 Praha 8, Czech Republic
[8] Centro Brasileiro de Pesquisas Físicas, R. Dr. Xavier Sigaud, 150 - Rio de Janeiro - RJ, 22290-180, Brazil
[9] Academic Department of Physics – Faculty of Sciences – Universidad Nacional de San Antonio Abad del Cusco (UNSAAC), Av. de la Cultura, 733, Pabellón C-358, Cusco, Peru
[10] Instituto de Física, Universidad Nacional Autónoma de México, Sendero Bicipuma, C.U., Coyoacán, 04510 Ciudad de México, CDMX, México
[11] Dipartimento di Fisica, Università degli Studi di Torino, Via Pietro Giuria 1, 10125, Torino, Italy
[12] RWTH Aachen University, Physics Institute 3, Otto-Blumenthal-Straße, 52074 Aachen, Germany
[13] University of Maryland, College Park, MD 20742, United States
[14] Durham University, Stockton Road, Durham, DH1 3LE, United Kingdom
[15] Astronomical Observatory, University of Warsaw, Aleje Ujazdowskie 4, 00478 Warsaw, Poland
[16] Facultad de Ciencias en Física y Matemáticas UNACH, Boulevard Belisario Domínguez, Km. 1081, Sin Número, Terán, Tuxtla Gutiérrez, Chiapas, México
[17] Facultad de Ciencias Exactas, Universidad Nacional de Salta, Avda. Bolivia N° 5150, (4400) Salta Capital, Argentina
[18] Department of Aerospace Science and Technology, Politecnico di Milano, Via Privata Giuseppe La Masa, 34, 20156 Milano MI, Italy
[19] Facultad de Ciencias Físico Matemáticas, Benemérita Universidad Autónoma de Puebla, C.P. 72592, México
[20] Instituto de Astronomia y Fisica del Espacio (IAFE, CONICET-UBA), Casilla de Correo 67 - Suc. 28 (C1428ZAA), Ciudad Autónoma de Buenos Aires, Argentina
[21] Universidad de Guadalajara, Blvd. Gral. Marcelino García Barragán 1421, Olímpica, 44430 Guadalajara, Jal., México
[22] Instituto de Física de São Carlos, Universidade de São Paulo, Avenida Trabalhador São-carlense, nº 400, Parque Arnold Schimidt - CEP 13566-590, São Carlos - São Paulo - Brasil
[23] INFN - Roma Tor Vergata and INAF-IAPS, Via del Fosso del Cavaliere, 100, 00133 Roma RM, Italy
[24] Dept. of Physics and CCTVal, Universidad Tecnica Federico Santa Maria, Avenida España 1680, Valparaíso, Chile
[25] Universität Würzburg, Institut für Theoretische Physik und Astrophysik, Emil-Fischer-Str. 31, 97074 Würzburg, Germany
[26] Department of Physics, and the Wisconsin IceCube Particle Astrophysics Center (WIPAC), University of Wisconsin, 222 West Washington Ave., Suite 500, Madison, WI 53703, United States
[27] TUBITAK Space Technologies Research Institute, ODTU Campus, 06800, Ankara, Turkey
[28] Friedrich-Alexander-Universität Erlangen-Nürnberg, Erlangen Centre for Astroparticle Physics, Erwin-Rommel-Str. 1, D 91058 Erlangen, Germany
[29] Tecnologico de Monterrey, Escuela de Ingeniería y Ciencias, Ave. Eugenio Garza Sada 2501, Monterrey, N.L., 64849, México
[30] Max-Planck-Institut für Kernphysik, P.O. Box 103980, D 69029 Heidelberg, Germany
[31] Università di Napoli "Federico II", Dipartimento di Fisica "Ettore Pancini", and INFN Napoli, Complesso Universitario di Monte Sant'Angelo - Via Cinthia, 21 - 80126 - Napoli, Italy
[32] University of Granada, Campus Universitario de Cartuja, Calle Prof. Vicente Callao, 3, 18011 Granada, Spain
[33] IFLP, Universidad Nacional de La Plata and CONICET, Diagonal 113, Casco Urbano, B1900 La Plata, Provincia de Buenos Aires, Argentina
[34] University of Utah, 201 Presidents' Cir, Salt Lake City, UT 84112, United States
[35] Michigan Technological University, 1400 Townsend Drive, Houghton, MI 49931, United States
[36] Dipartimento di Fisica e Astronomia "E. Majorana", Catania University and INFN, Catania, Italy

PoS(ICRC2021)714

[37] APC–IN2P3/CNRS, Université de Paris, Bâtiment Condorcet, 10 rue A.Domon et Léonie Duquet, 75205 PARIS CEDEX 13, France
[38] University of Leicester, University Road, Leicester LE1 7RH, United Kingdom
[39] Department of Physics, University of Trieste and INFN Trieste, via Valerio 2, I-34127, Trieste, Italy
[40]Centro de Investigación en Computación, Instituto Politécnico Nacional, Av. Juan de Dios Bátiz S/N, Nueva Industrial Vallejo, Gustavo A. Madero, 07738 Ciudad de México, CDMX, México
[41] Department of Physics and Mathematics, Universidad de Monterrey, Av. Morones Prieto 4500, San Pedro Garza García 66238, N.L., México
[42] Department of Physics and Astronomy, University of Alabama, Gallalee Hall, Tuscaloosa, AL 35401, United States
[43] Instituto de Tecnologías en Detección y Astropartículas (CNEA-CONICET-UNSAM), Av. Gral Paz 1499 - San Martín - Pcia. de Buenos Aires, Argentina
[44] Department of Physics, ETH Zurich, CH-8093 Zurich, Switzerland
[45] Instituto de Ciencias Nucleares, Universidad Nacional Autónoma de México (ICN-UNAM), Cto. Exterior S/N, C.U., Coyoacán, 04510 Ciudad de México, CDMX, México
[46] Departamento de Física, Facultad de Ciencias Básicas, Universidad Metropolitana de Ciencias de la Educación, Av. José Pedro Alessandri 774, Ñuñoa, Santiago, Chile
[47] Department of Physics, University of Seoul, 163 Seoulsiripdaero, Dongdaemun-gu, Seoul 02504, Republic of Korea
[48] Institut de recherche sur les lois fondamentales de l'Univers (IRFU), CEA, Université Paris-Saclay, F-91191 Gif-sur-Yvette, France
[49] Laboratoire Univers et Particules de Montpellier, CNRS, Université de Montpelleir, F-34090 Montpellier, France
[50] Instituto Nacional de Astrofísica, Óptica y Electrónica (INAOE), Luis Enrique Erro 1, Puebla, México